Likelihood Ratio-Based Distribution-Free EWMA Control Charts

CHANGLIANG ZOU

Nankai University, Tianjin, China

FUGEE TSUNG

Hong Kong University of Science and Technology, Clear Water Bay, Kowloon, Hong Kong

Nonparametric or distribution-free charts are useful in statistical process control when there is a lack of or limited knowledge about the underlying process distribution. Most existing approaches in the literature are for monitoring location parameters. They may not be effective with a change of distribution over time in many applications. This paper develops a new distribution-free control chart based on the integration of a powerful nonparametric goodness-of-fit test and the exponentially weighted moving-average (EWMA) control scheme. Benefiting from certain good properties of the test and the proposed charting statistic, our proposed control chart is fast in computation, convenient to use, and efficient in detecting potential shifts in location, scale, and shape. Thus, it offers robust protection against variation in various underlying distributions. Numerical studies and a real-data example show that the proposed approaches would be quite effective in industrial applications, particularly in start-up and short-run situations.

Key Words: Anderson-Darling Test; Change Point; Goodness of Fit; Self-Starting; Statistical Process Control; Weighted Empirical Distribution.

STATISTICAL process control (SPC) has been widely used to monitor various industrial processes. Most SPC applications assume that the quality of a process can be adequately represented by the distribution of a quality characteristic and the in-control (IC) and out-of-control (OC) distributions are the same with only differing parameters. While parametric methods are useful in certain applications, questions will always arise about the adequacy of those distributional assumptions and about the potential impact of misspecifications of distributions on charting performance. For example, univariate process data are often assumed to have normal distributions, although it is well recognized that, in many applications, particularly in start-up situations, the underlying process distribution is unknown and not normal, so that statistical properties of commonly used charts, designed to perform best under the normal distribution, could potentially be (highly) affected. Nonparametric or distribution-free charts are particularly useful in such situations. A chart is called distribution-free or nonparametric if its IC run-length distribution is the same for every continuous distribution (c.f., Chakraborti et al. (2001)).

In the last several years, nonparametric control charts have attracted much attention from researchers. Among others, for example, Bakir and Reynolds (1979) proposed a cumulative sum (CUSUM) chart for group observations based on the Wilcoxon signed-rank statistic. McDonald (1990) considered a CUSUM procedure for individual observations based on the statistics called "sequential ranks". An exponentially weighted moving-average (EWMA) chart for individual observations proposed by Hackl and Ledolter (1991) is constructed by the "standardized ranks" of observations, which is determined by IC distributions. If the distribution is not available, they recommended using the ranks in collected reference data instead. The non-

Dr. Zou is an Assistant Professor in the LPMC and School of Mathematical Sciences. His email is chlzou@yahoo.com.cn.

Dr. Tsung is a Professor in the Department of Industrial Engineering and Logistics Management. He is a Fellow of ASQ. His email is season@ust.hk.

parametric charts considered by Chakraborti et al. (2004, 2009) are based on the precedence test. Recently, a Shewhart-type chart and a scheme using change-point formulation based on the well-known Mann–Whitney test statistic were investigated by Chakraborti and Van de Wiel (2008) and Zhou et al. (2009), respectively. Hawkins and Deng (2010) considered a similar framework to that of Zhou et al. (2009) but focused on a direct nonparametric parallel of Hawkins et al. (2003) with modest computational needs. Jones et al. (2009) developed a rank-based distribution-free Phase I control scheme for subgroup location. Other developments include Albers and Kallenberg (2004) and Bakir (2004, 2006). A nice overview on the topic of univariate nonparametric control charts was presented by Chakraborti et al. (2001). In addition, nonparametric control charts in multivariate cases have been discussed by Liu (1995), Qiu and Hawkins (2001), and Qiu (2008).

Most of the approaches mentioned above focus on detecting shifts in location parameters (mean, median, or some percentiles of the distribution). Although the problem of monitoring the center or the location of a process is important in many applications, on-line monitoring of the change in an entire distribution is highly desirable because other distribution characteristics, such as the scale and shape, are also important quality indicators. For example, an increase in the variation usually corresponds to the process deterioration, which requires timely and proper preventive measures taken by practitioners. The problem of simultaneously monitoring the mean and variance has received attention in the literature on parametric control charts, e.g., see Chen et al. (2001), Hawkins and Zamba (2005), and the references therein.

In this paper, we study the Phase II method for nonparametrically monitoring distributional change. To be specific, we assume that there are m_0 independent and identically distributed (i.i.d.) historical (reference) observations $X_{-m_0+1}, \ldots, X_0$, and the tth future observation, X_t, collected over time, comes from the following change-point model:

$$X_t \overset{\text{i.i.d}}{\sim} \begin{cases} F_0(x), & \text{for } t = -m_0+1, \ldots, 0, 1, \ldots, \tau, \\ F_1(x), & \text{for } t = \tau+1, \ldots, \end{cases} \tag{1}$$

where τ is the unknown change point and $F_0 \neq F_1$ are the unknown IC and OC distribution functions. This is related to the goodness-of-fit (GOF) test problem in the nonparametric statistical inference context. The well-known tests include Kolmogorov–Smirnov, Anderson–Darling, and Cramér-von Mises test statistics (see Conover (1999) for an overview and references). Zhang (2002, 2006) proposed a new approach of parameterization to construct a general GOF test based on the nonparametric likelihood ratio. It not only generates the foregoing traditional tests but also produces new types of omnibus tests that are generally much more powerful than the old ones. We are interested in tackling the monitoring problem in Equation (1) using the nonparametric likelihood-ratio approach.

In this paper, we propose a new distribution-free control chart by adapting Zhang's (2002) testing approach to repeated sequential use. The proposed chart incorporates the exponential weights used in the EWMA scheme at different time points into the empirical distribution function of the collected observation over time and updates the unknown IC distribution estimation along with new observations, which serve the self-starting purpose. Simulation studies show that the proposed approach not only has at least comparable ability to detect shifts in location as the conventional schemes in the literature, but it is also superior to other nonparametric schemes in monitoring changes in scale in terms of average run length (ARL). As it avoids the need for a lengthy data-gathering step before charting (although it is generally necessary and advisable to collect a few preliminary stable observations by a Phase I analysis) and it does not require knowledge of the underlying distribution, the proposed control chart is particularly useful in start-up or short-run situations. A real-data example from manufacturing shows that it performs quite well in applications.

A New Distribution-Free Control Chart

In this section, a new nonparametric EWMA control chart combined with Zhang's (2002) GOF test is derived. Its determination of control limits and practical guidelines regarding design and computational issues are addressed in a latter section. Recall the model (1) and associated notation. Next, we elaborate on the individual observation model. The extension to the group case will be presented later. To facilitate the derivation of the proposed charting statistic, we start by supposing the $F_0(x)$ is known and we let $X_1, \ldots, X_n$ be a fixed random sample from X, which is a continuous random variable with the distribution function $F(x)$. We want to test the null hypothesis H_0 that $F(x) = F_0(x)$ for all $x \in (-\infty, \infty)$ against H_1 that $F(x) \neq F_0(x)$ for some $x \in (-\infty, \infty)$. Testing H_0 against H_1 is equivalent to testing H_{0u} that $F(u) = F_0(u)$ against H_{1u} that $F(u) \neq F_0(u)$ for every $u \in (-\infty, \infty)$.

Zhang (2002) introduced a parameterization approach to establish powerful GOF tests based on the following log-likelihood ratio (c.f., Einmahl and McKeague (2003) and the references therein)

$$G_u = n\left\{F_n(u)\ln\left(\frac{F_n(u)}{F_0(u)}\right) + [1 - F_n(u)]\ln\left(\frac{1 - F_n(u)}{1 - F_0(u)}\right)\right\}, \quad (2)$$

where the original sample is regarded as a binary sample with $F_n(u)$ probability of success and $F_n(u)$ is the empirical distribution function (e.d.f.) of the sample $\{X_1, \ldots, X_n\}$, say $F_n(u) = n^{-1}\sum_{j=1}^{n} I_{\{X_j \leq u\}}$, where $I_{\{.\}}$ is the indicator function. Then some powerful test statistics can be produced based on this log-likelihood ratio. Note that this ratio is only evaluated at a single point u but, as mentioned before, we are testing $F(u) = F_0(u)$ for every $u \in (-\infty, \infty)$. An intuitive way is to combine all of the log-likelihood ratios evaluated at the observations $X_i, i = 1, \ldots, n$, by incorporating an appropriate weight (α_i) for each X_i, say, $Z = \sum_{i=1}^{n} \alpha_i G_{X_i}$.

One of most powerful tests introduced by Zhang (2002) is to use $\alpha_i = [F_n(X_i)(1 - F_n(X_i))]^{-1}$, which leads to

$$Z_A = \sum_{i=1}^{n} \omega_i \left\{\frac{1}{1 - F_n(X_i)}\ln\left(\frac{F_n(X_i)}{F_0(X_i)}\right) + \frac{1}{F_n(X_i)}\ln\left(\frac{1 - F_n(X_i)}{1 - F_0(X_i)}\right)\right\}, \quad (3)$$

with $\omega_i = 1$ for all i and large values of Z_A reject the null hypothesis. Note that the function $[F_n(x)(1 - F_n(x))]^{-1}$ attains its minimum at $F_n(x) = 1/2$, that is, when x is the median of the sample. Intuitively speaking, the more extreme observations (far way from the median), corresponding to larger values of α_i, are more informative for indicating the violation of H_0 and the weights may be accordingly chosen larger. This test is an analog of the traditional Anderson–Darling rank test (Anderson (1962)), but it is much more powerful than the Anderson–Darling test. In what follows, we focus on this type of test.

A naive method that comes to mind for on-line detection is to use the current individual observation to construct the Z_A ($n = 1$) test, say, a Shewhart-type chart. However, this would be very inefficient with moderate and small changes because it completely ignores the past observations. As an alternative, we consider the following weighted empirical distribution function at any point, u,

$$F_n^{(\lambda)}(u) = a_{\lambda,n}^{-1}\sum_{j=1}^{n}(1 - \lambda)^{n-j} I_{\{X_j \leq u\}}, \quad (4)$$

with

$$a_{\lambda,n} = \sum_{j=1}^{n}(1 - \lambda)^{n-j},$$

where λ is a weighting parameter commonly used in the EWMA chart. Note that $F_n^{(\lambda)}(u)$ combines the exponential weighting scheme used in EWMA at different time points by the term $(1 - \lambda)^{n-j}$ and the traditional e.d.f. This is analogous to the approach used in the nonparametric kernel density estimation where the neighborhoods of objective points have more weight.

When the tth future observation, X_t, is collected, in light of $F_n^{(\lambda)}(u)$, we propose a new charting statistic, Z_t, by replacing $F_n(X_i)$ with $F_i^{(\lambda)}(X_i)$ and taking $\omega_i = \lambda(1 - \lambda)^{t-i}$ in Z_A,

$$Z_t = \sum_{i=1}^{t}\lambda(1 - \lambda)^{t-i} \cdot \left\{\frac{1}{1 - F_i^{(\lambda)}(X_i)}\ln\left(\frac{F_i^{(\lambda)}(X_i)}{F_0(X_i)}\right) + \frac{1}{F_i^{(\lambda)}(X_i)}\ln\left(\frac{1 - F_i^{(\lambda)}(X_i)}{1 - F_0(X_i)}\right)\right\},$$

which is equivalent to the following formulation:

$$Z_t = (1 - \lambda)Z_{t-1} + \lambda Y_t, \quad t = 1, 2, \ldots, \quad (5)$$

where

$$Y_t = \frac{1}{1 - F_t^{(\lambda)}(X_t)}\ln\left(\frac{F_t^{(\lambda)}(X_t)}{F_0(X_t)}\right) + \frac{1}{F_t^{(\lambda)}(X_t)}\ln\left(\frac{1 - F_t^{(\lambda)}(X_t)}{1 - F_0(X_t)}\right)$$

and $Z_0 = 0$. Obviously, this test makes use of all available observations up to the current time point, t, and different observations are weighted as in an EWMA chart (i.e., more recent observations have more weight and the weight changes exponentially over time). The form of Z_t in Equation (5) operates in a similar way to the conventional parametric EWMA chart for normal variables (Lucas and Saccucci (1990)). Note that the smoothing parameter λ is used in both the ω_i and the weighted e.d.f. $F_n^{(\lambda)}$ to get rid of certain effects of historical information.

By setting $\omega_i = \lambda(1-\lambda)^{t-i}$, we combine all the Y_ts with an exponential weighting strategy because more recent observations may indicate the change more accurately and easily. Similarly, using $F_n^{(\lambda)}$ results in a more updated estimate of F_1 and thus also plays an important role in Z_t. We should emphasize that, unlike the recursive form in the conventional parametric EWMA chart, Equation (5) is not recursive because there is no recursive expression for calculating Y_t. That is, the computational effort of calculating Y_t grows sequentially with time t. The detailed discussion about computational issues is provided in the next section.

Up to now, we assume that $F_0(x)$ is known, which is equivalent to saying that m_0 is sufficiently large. If so, we could directly replace $F_0(X_t)$ in Equation (5) with the e.d.f. $F_{-m_0,0}(X_t) = m_0^{-1}\sum_{j=-m_0+1}^{0} I_{\{X_j \le X_t\}}$. However, when m_0 is not large, there would be considerable uncertainty in the distribution estimation, which in turn would distort the IC run-length distribution of the control chart. Even if the control limit of the chart was adjusted properly to obtain the desired IC run-length behavior, its OC run length would still be severely compromised (cf., Jones (2002)). This is essentially analogous to the estimated parameters problem in the context of parametric control charts (see Jensen et al. (2006) for an overview).

To deal with the situation when a sufficiently large reference dataset is unavailable, self-starting methods that handle sequential monitoring by simultaneously updating parameter estimates and checking for OC conditions have been developed accordingly (see Hawkins (1987), Quesenberry (1991)). To this end, using $F_{-m_0,t-1}(X_t) = (m_0+t-1)^{-1}\sum_{j=-m_0+1}^{t-1} I_{\{X_j \le X_t\}}$ to replace $F_0(X_t)$ in Z_t for $t \ge 1$ yields our suggested charting statistics with m_0 reference observations,

$$\tilde{Z}_t = (1-\lambda)\tilde{Z}_{t-1} + \lambda \tilde{Y}_t, \tag{6}$$

with

$$\tilde{Y}_t = \frac{1}{1-F_t^{(\lambda)}(X_t)} \ln\left(\frac{F_t^{(\lambda)}(X_t)}{F_{-m_0,t-1}(X_t)}\right) + \frac{1}{F_t^{(\lambda)}(X_t)} \ln\left(\frac{1-F_t^{(\lambda)}(X_t)}{1-F_{-m_0,t-1}(X_t)}\right), \tag{7}$$

and the corresponding control chart triggers a signal if

$$\tilde{Z}_t > L_t,$$

where $L_t > 0$ is a sequence of control limits chosen to achieve a specific IC run-length distribution.

This chart is referred to as the nonparametric likelihood-ratio EWMA (NLE) chart hereafter. It is able to detect both the increase and decrease in location, scale, or even in shape parameters (say, "two-sided" in the parameter). The time-varying control limits L_ts are used because the IC sampling distribution of Z_t converges slowly, especially with small m_0. The probabilities of false alarms from the chart may increase dramatically after short runs if we use a fixed control limit. The approach of using dynamic control limits is originally proposed by Lai (1995) and has been successfully formalized and utilized by Hawkins et al. (2003) in the parametric change-point–based control charts with unknown IC parameters.

Intuitively speaking, $\tilde{Z}_t$ is nonparametric because the statistic $\tilde{Y}_t$ only uses the rank information of X_t's but not the magnitudes of X_ts. In fact, from the definition of $\tilde{Z}_t$, we can see that up to $t \ge 1$, the IC run-length distribution of the NLE chart is determined by the densities $f_{\tilde{Y}_1}, f_{\tilde{Y}_2|\tilde{Y}_1}, \ldots, f_{\tilde{Y}_t|\tilde{Y}_i, i<t}$, where $f_{x|y_1,\ldots,y_k}$ denotes the conditional density of x given $y_1,\ldots,y_k$. Note that $\{\tilde{Y}_1,\ldots,\tilde{Y}_t\}$ are determined by the ranks of $\{X_1,\ldots,X_t\}$ in the pooled sample, $\{X_{-m_0+1},\ldots,X_t\}$, which are free of the underlying IC process distribution because $X_{-m_0+1},\ldots,X_t$ are i.i.d. distributed from F_0. By deduction, we know that, $f_{\tilde{Y}_1}$, $f_{\tilde{Y}_2|\tilde{Y}_1}, \ldots, f_{\tilde{Y}_t|\tilde{Y}_i, i<t}$ are also free of $F_0(x)$, which yields the following result: the NLE chart is distribution-free, i.e., its IC run-length distribution is the same for all continuous process distributions. This is particularly useful in determining the control limits because, for any continuous process distribution, the L_t's are the same for achieving the desired IC run-length distribution. In other words, the control limits can be chosen independently of F_0 to give a desired run-length distribution.

In practice, it might be more convenient to plot the normalized statistic, $\tilde{Z}_t/L_t$, over t in a control chart. In such cases, the normalized control limit is a constant 1. The determination of L_t and several other issues on implementing the NLE chart are discussed in the next section.

Design and Implementation of the Proposed Scheme

Determining Control Limits

Like the analog Z_A, the null distribution of the proposed charting statistic, $\tilde{Z}_t$, is discrete for any given t. Therefore, theoretically, it can be obtained by enumerating all possible values of the statistics. This is not feasible unless t and m_0 are both small. Even though we obtain the full distribution for any given λ, t, and m_0, the IC run-length distribution of the NLE chart is still unknown to us because it depends on the conditional distribution, say, $f_{\tilde{Z}_t|\tilde{Z}_i, i\leq t-1}$. Similar to Hawkins et al. (2003) and Zhou et al. (2009), for a given false-alarm probability, α, which corresponds to the IC ARL (denoted as ARL_0 for abbreviation hereafter), the control limits, L_t, can be approximated by values satisfying

$$\alpha = \begin{cases} \Pr\left(\tilde{Z}_t > L_t \middle| \tilde{Z}_i \leq L_i, 1 \leq i < t\right) & \text{for } t > 1, \\ \Pr\left(\tilde{Z}_1 > L_1\right). \end{cases} \tag{8}$$

Of course, the above probabilities should be interpreted as relative frequencies in many simulation replications. Note that, in the case that F_0 is assumed known, the procedure above is still applicable except that we use the formula (5) and Z_t instead of the formula (6) and $\tilde{Z}_t$, respectively.

Although the NLE chart is a self-starting scheme and thus can be implemented at the start-up of a process, we believe that starting testing with too small an m_0 is not a good idea. Too small an m_0 would result in a severe "masking effect" if a short-run change occurred. Rather, we suggest that a practitioner should gather a modest number of observations through a Phase I study to get at least an initial verification that the process was actually stable, and only then start the formal NLE chart. Therefore, similar to Hawkins et al. (2003), we suggest collecting at least $m \geq 25$ (of course the more the better) historical observations before monitoring. Our empirical results show that, to get a satisfactory monitoring performance, it may require 50–100 IC observations (say, $m_0 + \tau \geq 50$) before the change actually occurred.

Note that the possible values of $\tilde{Z}_t$ for very small t, say $t = 1$ or 2, are very limited when m_0 is small, so it is not likely to obtain the L_t for $t = 1, 2$ to achieve a desired α. More specifically, by examining the definition of $F_t^{(\lambda)}$ in Equation (4), we can see that there are only m_0 possible values of $\tilde{Z}_t$ for $t = 1$ but at least about cm_0^2 (for a value $0 < c < 1$) possible values of $\tilde{Z}_t$ for $t = 2$ given m_0. To resolve the problem of finding L_1 or L_2 with too small m_0, we suggest taking two of m_0 historical observations as the pseudo-future observations, without loss of generality, using the last two historical observations X_{-1} and X_0. Then calculate the corresponding charting statistic $\tilde{Z}_t$ for $t = -1, 0$ but to start testing after the first actual Phase II observation is obtained. That is to say, the first two pseudo-$\tilde{Z}_t$'s are used for making the possible values of $\tilde{Z}_1$ and $\tilde{Z}_2$ be sufficient to obtain the control limits. The following tabulated control limits and our main simulation are all in line with this modification.

Based on the empirical results in Hawkins et al. (2003) as well as our numerical study, the L_t would gradually converge to a constant when t increases. Thus, we suggest computing about the first $1/\alpha$ control limits and then using the last one of this sequence or searching for a constant through independent simulations to approximate the remaining control limits. In addition, in computing each L_t, about 50,000 replications should be enough to obtain reliable approximations. For instance, if $\text{ARL}_0 = 200$, we need to compute the first 200 control limits, which requires about 140,000 sequences, so that there are about 50,000 sequences left for computing the 200th control limit, L_{200}. Today's computing equipment and software make it easy to compute and store such control limits for on-line automatic detection use.

Table 1 shows the control limits of the NLE chart for α values of 0.005, 0.0027, and 0.002, corresponding to ARL_0 of 200, 370, and 500, when F_0 is known (using formula (5)) or m_0 is sufficiently large (using formula (7)). The missing values in Table 1 can be safely replaced by the value immediately above in the same column. Our numerous simulation experiments highlight that these control limits perform reasonably well as long as $m_0 \geq 2000$. Note that this number requirement is similar to Jones et al.'s (2001) recommendation for the traditional EWMA chart with estimated parameters to achieve the desire level of IC performance. Table 2 presents the control limits of the NLE chart for ARL_0 of 370 and 500, with various combinations of (λ, m_0). It is worth emphasizing again that the control limits tabulated in these tables can be used for any continuous distribution because the NLE is completely distribution free. We do not provide a regression formula that approximates the control limits in Tables 1 and 2 as in Hawkins et al. (2003) and Hawkins and Zamba (2005), as the data in our table cannot fit well using a simple regression. However, the tabulated data can be easily incorporated into computer programs, where storing such data is a trivial task. The computer code in Fortran for implementing the proposed scheme, including the

TABLE 1. The Control Limits L_t of the NLE Chart When F_0 Is Know

	$\lambda = 0.05$			$\lambda = 0.1$			$\lambda = 0.2$		
ARL_0	200	370	500	200	370	500	200	370	500
t									
1	9.232	10.441	11.111	9.246	10.531	11.038	9.132	10.422	11.037
2	12.190	13.778	15.044	11.646	13.338	14.546	10.730	12.309	13.002
3	13.187	15.308	16.547	12.231	14.100	15.431	10.405	12.008	12.987
4	13.381	15.864	17.081	12.018	14.088	15.268	9.584	11.134	12.044
5	13.406	15.890	17.159	11.557	13.718	14.746	8.783	10.147	10.862
6	13.205	15.774	17.077	11.072	13.140	14.105	8.087	9.354	10.053
7	12.913	15.492	16.691	10.482	12.473	13.494	7.460	8.599	9.303
8	12.625	15.133	16.383	9.937	11.834	12.720	7.015	8.079	8.640
9	12.287	14.783	15.872	9.402	11.190	12.085	6.597	7.591	8.165
10	11.983	14.332	15.468	8.932	10.568	11.388	6.319	7.317	7.685
11	11.630	13.920	15.096	8.539	10.093	10.839	6.083	6.969	7.384
12	11.286	13.557	14.663	8.157	9.613	10.312	5.910	6.715	7.165
13	10.991	13.117	14.265	7.804	9.171	9.850	5.755	6.621	7.006
14	10.675	12.772	13.820	7.510	8.776	9.436	5.619	6.445	6.749
15	10.395	12.393	13.474	7.213	8.410	9.052	5.542	6.329	6.671
16	10.131	12.060	13.030	6.945	8.106	8.756	5.430	6.223	6.615
17	9.829	11.712	12.718	6.729	7.904	8.437	5.380	6.146	6.601
18	9.601	11.390	12.329	6.513	7.579	8.095	5.323	6.078	6.433
19	9.323	11.121	11.994	6.330	7.324	7.863	5.218	6.000	6.402
20	9.092	10.788	11.660	6.181	7.160	7.636	5.204	5.962	6.432
22	8.624	10.242	11.011	5.924	6.809	7.300	5.126	5.937	6.277
24	8.222	9.715	10.463	5.622	6.514	7.051	5.123	5.891	6.244
26	7.875	9.249	9.952	5.431	6.360	6.824	5.076	5.877	6.217
28	7.531	8.864	9.495	5.301	6.176	6.654	5.072	5.860	6.191
30	7.179	8.470	9.159	5.157	6.013	6.364	5.067	5.842	6.186
35	6.545	7.720	8.254	4.893	5.746	6.156	5.058	5.837	6.178
40	6.071	7.131	7.592	4.761	5.595	5.953	5.050	5.799	6.173
50	5.305	6.279	6.701	4.608	5.442	5.826	5.048	5.792	6.167
60	4.840	5.712	6.147	4.552	5.322	5.710	5.044	5.785	6.160
70	4.544	5.410	5.784	4.536	5.313	5.693	5.039	5.777	6.156
80	4.343	5.195	5.530	4.528	5.299	5.674	5.035	5.771	6.151
90	4.257	5.053	5.440	4.513	5.290	5.662	5.030	5.766	6.144
115	4.051	4.868	5.268	4.502	5.285	5.650	5.027	5.761	6.140
140	4.032	4.797	5.221	4.496	5.278	5.642	5.025	5.754	6.138
165	4.025	4.794	5.209	4.491	5.272	5.638	5.023	5.745	6.136
190	4.023	4.787	5.182	4.486	5.267	5.635	5.021	5.732	6.134
240	4.022	4.778	5.179	4.482	5.257	5.631	5.020	5.729	6.133
290	4.020	4.770	5.177	4.480	5.248	5.629	5.018	5.726	6.132
390		4.759	5.175		2.244	5.627		5.724	6.130
490			5.174			5.625			6.129

TABLE 2. The Control Limits L_t of the NLE Chart with Various Values of m_0

	$m_0 = 25$				$m_0 = 50$			
	$\lambda = 0.05$		$\lambda = 0.1$		$\lambda = 0.05$		$\lambda = 0.1$	
ARL_0	370	500	370	500	370	500	370	500
t								
1	10.786	11.365	9.861	10.347	13.303	13.861	12.124	12.746
2	11.044	11.688	9.669	10.334	13.358	14.228	11.802	12.519
3	11.001	11.681	9.236	9.858	13.256	14.236	11.255	11.996
4	10.856	11.627	8.837	9.437	12.916	14.027	10.690	11.316
5	10.551	11.313	8.294	8.842	12.605	13.735	10.037	10.628
6	10.209	11.041	7.744	8.344	12.253	13.284	9.406	10.048
7	9.878	10.619	7.230	7.849	11.905	12.877	8.849	9.437
8	9.529	10.301	6.777	7.352	11.498	12.401	8.343	8.844
9	9.179	9.852	6.353	6.859	11.095	12.022	7.842	8.271
10	8.816	9.499	5.983	6.468	10.708	11.608	7.362	7.813
11	8.505	9.149	5.665	6.047	10.271	11.180	6.974	7.387
12	8.153	8.758	5.339	5.726	9.908	10.767	6.568	7.030
13	7.828	8.411	5.068	5.414	9.551	10.404	6.246	6.661
14	7.522	8.091	4.834	5.168	9.218	9.986	5.926	6.324
15	7.240	7.791	4.618	4.933	8.870	9.598	5.676	6.062
16	6.952	7.498	4.416	4.732	8.575	9.283	5.433	5.792
17	6.692	7.193	4.243	4.520	8.261	8.949	5.224	5.571
18	6.432	6.927	4.087	4.386	7.964	8.612	5.065	5.344
19	6.205	6.669	3.956	4.241	7.698	8.340	4.858	5.180
20	5.968	6.425	3.853	4.081	7.426	8.047	4.705	5.030
22	5.560	5.993	3.655	3.874	6.926	7.497	4.454	4.722
24	5.179	5.586	3.485	3.713	6.484	7.005	4.260	4.479
26	4.844	5.207	3.391	3.595	6.110	6.561	4.120	4.336
28	4.546	4.878	3.307	3.499	5.741	6.186	3.972	4.205
30	4.293	4.579	3.253	3.449	5.423	5.836	3.895	4.113
35	3.767	4.032	3.173	3.370	4.758	5.145	3.742	3.943
40	3.370	3.583	3.162	3.366	4.285	4.587	3.697	3.888
50	2.921	3.119	3.245	3.403	3.668	3.890	3.678	3.908
60	2.734	2.895	3.345	3.553	3.315	3.556	3.752	3.922
70	2.660	2.820	3.465	3.675	3.178	3.386	3.778	3.981
80	2.663	2.846	3.570	3.782	3.103	3.290	3.841	4.072
90	2.712	2.916	3.672	3.896	3.092	3.283	3.891	4.172
115	2.892	3.088	3.867	4.128	3.172	3.389	4.053	4.266
140	3.085	3.307	3.989	4.256	3.291	3.500	4.140	4.378
165	3.265	3.466	4.086	4.359	3.402	3.634	4.243	4.484
200	3.436	3.692	4.231	4.463	3.538	3.832	4.345	4.605
250	3.608	3.878	4.334	4.682	3.712	3.987	4.481	4.714
370	3.820	4.285	4.547	4.778	3.886	4.331	4.617	4.923
500	4.103	4.509	4.705	5.061	3.995	4.559	4.745	5.065

TABLE 2. *Continued*

	$m_0 = 100$				$m_0 = 200$			
	$\lambda = 0.05$		$\lambda = 0.1$		$\lambda = 0.05$		$\lambda = 0.1$	
ARL_0	370	500	370	500	370	500	370	500
t								
1	15.057	16.062	13.721	14.416	16.057	16.756	14.827	15.747
2	15.071	15.983	13.179	14.285	15.927	16.876	14.056	15.016
3	14.802	15.867	12.405	13.503	15.719	16.803	13.323	14.274
4	14.514	15.767	11.832	12.842	15.386	16.463	12.622	13.519
5	14.212	15.443	11.101	12.193	14.958	16.150	11.905	12.762
6	13.723	14.880	10.377	11.412	14.517	15.668	11.206	12.016
7	13.332	14.530	9.830	10.718	14.133	15.248	10.553	11.336
8	12.843	14.016	9.241	10.052	13.636	14.768	9.949	10.684
9	12.449	13.623	8.728	9.440	13.202	14.295	9.416	10.108
10	12.024	13.135	8.260	8.866	12.751	13.854	8.836	9.581
11	11.566	12.668	7.826	8.429	12.325	13.466	8.393	9.004
12	11.123	12.209	7.454	7.977	11.930	13.050	7.976	8.524
13	10.763	11.720	7.093	7.585	11.562	12.597	7.583	8.116
14	10.403	11.366	6.773	7.189	11.169	12.163	7.283	7.878
15	10.061	10.957	6.473	6.895	10.835	11.698	7.007	7.446
16	9.707	10.551	6.256	6.641	10.477	11.283	6.747	7.195
17	9.396	10.204	6.005	6.339	10.134	10.916	6.505	6.928
18	9.095	9.866	5.776	6.115	9.799	10.597	6.323	6.760
19	8.779	9.563	5.614	5.913	9.529	10.246	6.117	6.541
20	8.519	9.238	5.436	5.753	9.246	9.956	5.958	6.332
22	8.002	8.648	5.131	5.479	8.696	9.360	5.662	6.001
24	7.524	8.160	4.944	5.218	8.234	8.863	5.460	5.760
26	7.121	7.679	4.784	5.045	7.819	8.409	5.257	5.592
28	6.746	7.239	4.603	4.890	7.418	7.984	5.114	5.394
30	6.410	6.881	4.477	4.790	7.095	7.586	4.994	5.274
35	5.683	6.054	4.296	4.539	6.359	6.749	4.722	5.048
40	5.126	5.472	4.188	4.436	5.803	6.164	4.653	4.917
50	4.404	4.706	4.075	4.320	4.986	5.337	4.512	4.772
60	3.977	4.236	4.102	4.328	4.560	4.826	4.498	4.740
70	3.749	3.959	4.110	4.346	4.251	4.503	4.442	4.707
80	3.598	3.863	4.173	4.391	4.086	4.359	4.469	4.717
90	3.528	3.766	4.187	4.433	3.967	4.255	4.488	4.767
115	3.510	3.759	4.273	4.531	3.887	4.161	4.528	4.843
140	3.567	3.811	4.342	4.587	3.925	4.167	4.575	4.855
165	3.676	3.882	4.408	4.661	3.943	4.212	4.597	4.877
200	3.749	3.979	4.455	4.765	3.986	4.268	4.645	4.894
250	3.858	4.148	4.588	4.878	4.114	4.331	4.704	4.974
370	4.090	4.380	4.679	5.051	4.233	4.502	4.776	5.164
500	4.187	4.549	4.723	5.124	4.302	4.689	4.832	5.207

procedures for finding the control limits, is available from the authors on request.

Choosing λ

In general, a smaller λ leads to a quicker detection of smaller shifts (c.f., e.g., Lucas and Saccucci (1990)). This statement is still valid with the NLE chart. Here we present some simulation results regarding the effect of λ on the performance of NLE. Because of the importance of the monitoring of mean change for the normal distribution, we evaluate the OC ARL (denoted as ARL_δ) under the scenario $N(0, 1)$ versus $N(\delta, 1)$ for $\delta \neq 0$. We only report the steady-state ARL_δ behavior here. To evaluate the ARL_δ, any series in which a signal occurs before the $(\tau + 1)$-th observation is discarded (Hawkins et al. (2003)). $\tau = 50$ and $\text{ARL}_0 = 370$ are fixed in this example, and 20,000 replications are used. Figures 1(a) and 1(b) show the ARL_δs (in log scale) of NLE with the λ values of 0.05, 0.1, 0.2, and 0.5 when F_0 is known and $m_0 = 100$, respectively. We can clearly see that, in both cases, a smaller λ leads to a quicker detection of smaller shifts and a larger λ performs better in detecting larger shifts. This is consistent with the properties of the conventional EWMA chart (Lucas and Saccucci (1990)) and its self-starting version (Quesenberry (1995)). Based on our empirical results, we suggest choosing $\lambda \in [0.05, 0.2]$, which is a reasonable choice. To obtain more robust protection against various shift sizes, the adaptive EWMA (Capizzi and Masarotto (2003)) or multi-EWMA (Han et al. (2007)) schemes may be extended to the NLE chart. These studies are beyond the scope of this paper but could be subjects of future research.

Computation

In comparison with Zhou et al.'s (2009) change-point control chart, the NLE chart does not require binary segmentation. At any time point t, it involves, at most, order $t-1$ computations (i.e., comparing X_t with $X_{-m_0+1}, \ldots X_{t-1}$), and thus the computational task is actually quite simple. Using the dichotomy method and updating the ranks of $X_{-m_0+1}, \ldots X_t$ in a recursive manner could further alleviate the computational burden. For instance, when $\text{ARL}_0 = 200$, it takes about 3 minutes to search for the control limits based on 200,000 simulations, using a Pentium 2.4MHz CPU.

Post-Signal Diagnostic

In the practice of quality control, in addition to detecting a process change quickly, it is also critical to diagnose the change and to identify if there has been a shift in location, scale, or both after an OC signal occurs. A diagnostic aid to locate the change point in the process and to isolate the type of parameter change will help an engineer to identify and eliminate the root cause of a problem quickly and easily.

An estimate of the change point based on the non-

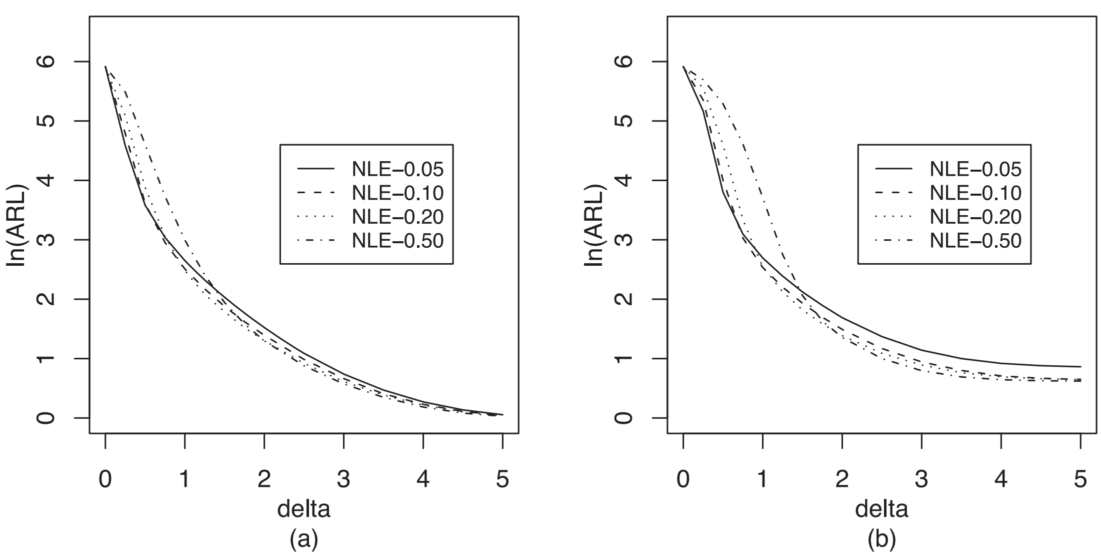

FIGURE 1. The Steady-State OC ARL Curves of the NLE Charts with Various Values of λ for Monitoring $N(0, 1)$ Versus $N(\delta, 1)$ When: (a) F_0 Is Known; (b) $m_0 = 100$.

parametric test Z_A is proposed to assist in the diagnosis of our NLE chart. We assume that the chart signals at the kth observation, i.e., there are m_0 historical IC observations and k future observations, and a shift occurred after the τth sample ($0 \leq \tau < k$) as illustrated by model (1). Given an estimate of change point v, we can derive the following generalized version of Z_A:

$$\begin{aligned} Z_A(v,k) &= \sum_{i=v+1}^{k} \left\{ \frac{1}{1 - F_{v,k}(X_i)} \ln\left(\frac{F_{v,k}(X_i)}{F_{-m_0,v}(X_i)}\right) \right. \\ &\quad \left. + \frac{1}{F_{v,k}(X_i)} \ln\left(\frac{1 - F_{v,k}(X_i)}{1 - F_{-m_0,v}(X_i)}\right) \right\}, \end{aligned} \tag{9}$$

where $F_{k_1,k_2}(X_i)$ is defined by

$$(k_2 - k_1)^{-1} \sum_{j=k_1+1}^{k_2} I_{\{X_j \leq X_i\}}$$

as before. Actually, the $Z_A(v,k)$ can intuitively be understood as a test statistic based on Z_A in Equation (3) for testing if the sample $\{X_i, i = v+1, \ldots, k\}$ has the same distribution as $F_{-m_0,v}(\cdot)$, where $F_{-m_0,v}$ can be regarded as an estimate of F_0. Then our suggested estimator of the change point, τ, is given by

$$\widehat{\tau} = \arg\max_{0 \leq v < k} \{Z_A(v,k)\}. \tag{10}$$

Such type of estimator is often used for off-line nonsequential change-point detection in the literature (c.f., Csorgo and Horvath (1998)). In this paper, we utilize it in an on-line SPC application. Among others, Pignatiello and Samuel (2001), Hawkins and Zamba (2005), and Zou et al. (2007) have used analogous estimators based on parametric generalized likelihood ratios in various monitoring problems. Under some mild conditions, we can have asymptotic results on the consistency of this change-point estimator, which ensure that it is asymptotically effective. Because this is out of the scope of this paper, we will discuss this problem in a separate paper. We will demonstrate the effectiveness of $\widehat{\tau}$ by simulation in the next section.

After an estimate of the shift location is obtained, we have $(k - \widehat{\tau})$ OC observations that have shifts in their distributions. Among these $(k - \widehat{\tau})$ observations, a few might actually be IC observations, because $\widehat{\tau}$ is only an estimator of the true shift location τ. At first glance, our proposed method based on an omnibus chart seems not able to diagnose whether a shift in location or scale occurred. However, as Reynolds and Stoumbos (2005) pointed out, the control charts used as diagnostic aids do not necessarily have to be the same control charts that were used to determine when to signal. Similar arguments can also be found in Hawkins and Zamba (2005), where two parametric tests are used to determine if the shift comes from the mean or the variance. Thus, in this paper, we propose using a nonparametric test method as an auxiliary tool to determine which parameters have changed after the chart has triggered a signal.

We suggest using the following nonparametric two-sample tests: the well-known Wilcoxon rank sum test (or called Mann–Whitney–Wilcoxon test; e.g., see Conover (1999)) for location and the aligned rank scale test (Fligner and Killeen (1976)), denoted as T_W and T_A respectively. To be specific,

$$T_W = \sum_{i=-m_0+1}^{\widehat{\tau}} \sum_{j=\widehat{\tau}+1}^{k} I_{\{X_j \leq X_i\}}. \tag{11}$$

Denote $X_j^* = X_j - \widehat{\theta}_{-m_0,\widehat{\tau}}$ for $j = -m_0+1, \ldots, \widehat{\tau}$ and $Y_j^* = X_j - \widehat{\theta}_{\widehat{\tau},k}$ for $j = \widehat{\tau}+1, \ldots, k$, where $\widehat{\theta}_{-m_0,\widehat{\tau}}$ and $\widehat{\theta}_{\widehat{\tau},k}$ are the sample medians of the samples before and after $\widehat{\tau}$. Then T_A is defined as

$$T_A = \sum_{j=\widehat{\tau}+1}^{k} \left(\Phi^{-1}\left(\frac{R(|Y_j^*|)}{2(n+1)} + \frac{1}{2}\right)\right)^2, \tag{12}$$

where $R(|Y_j^*|)$'s denote the rankings that are over the absolute values of the aligned observations $\{X_{-m_0+1}^*, \ldots, X_{\widehat{\tau}}^*, Y_{\widehat{\tau}+1}^*, \ldots, Y_k^*\}$ and $\Phi^{-1}(\cdot)$ is the inverse of the standard normal cumulative distribution function. This scale test possessed both robustness of validity and power in the study by Conover et al. (1981) and was one of the few tests of their study that they recommended for general use. One may obtain the critical values of T_W and T_A by means of simulation methods or normal approximations (c.f., Conover (1999)). We will study their performance in the next section. As a side note, using the traditional two-sample t- and F-tests for location and dispersion parameters, respectively, suggested by Hawkins and Zamba (2005), may be an alternative choice but we do not elaborate on them here.

Group Observations

When a group of g observations, say $\{X_{j1}, \ldots, X_{jg}\}$, are taken sequentially from the process at each time point, the NLE chart can be readily defined in a similar way to Equation (6) by using the following modified (weighted) empirical distribution function:

$$F^{(g)}_{-m_0,k}(u) = \frac{1}{(k+m_0)g} \sum_{j=-m_0+1}^{k} \sum_{i=1}^{g} I_{\{X_{ji} \le u\}}$$

$$F^{(\lambda,g)}_{k}(u) = a^{-1}_{\lambda,k,g} \sum_{j=1}^{k} (1-\lambda)^{k-j} \sum_{i=1}^{g} I_{\{X_{ji} \le u\}},$$

with

$$a_{\lambda,k,g} = g \sum_{j=1}^{k} (1-\lambda)^{k-j}.$$

Then the NLE charting statistic for group observation is given by Equation (6) with

$$\tilde{Y}^{(g)}_t = \sum_{i=1}^{g} \frac{1}{1-F^{(\lambda,g)}_t(X_{ti})} \ln\left(\frac{F^{(\lambda,g)}_t(X_{ti})}{F^{(g)}_{-m_0,t-1}(X_{ti})}\right) + \frac{1}{F^{(\lambda,g)}_t(X_{ti})} \ln\left(\frac{1-F^{(\lambda,g)}_t(X_{ti})}{1-F^{(g)}_{-m_0,t-1}(X_{ti})}\right),$$

instead of $\tilde{Y}_t$, where we still follow the principle that the observations in the same group have the same weights and more recent groups have more weight.

Numerical Performance Assessment

We present some simulation results in this section on the numerical performance of the proposed NLE procedure. Because a similar conclusion holds for other cases, throughout this section, we only present the results when $\mathrm{ARL}_0 = 370$ for illustration. Some other results with other commonly used ARL_0's, such as 200 or 500, are available from the authors on request. All the ARL results in this section are obtained from 20,000 replications unless indicated otherwise.

Comparisons between NLE and Conventional Parametric Charts

First, we compare the performance of NLE with conventional parametric charts designed under the normality assumption. Among others, the univariate nonnormality problem was studied by Borror et al. (1999) and Stoumbos and Reynolds (2000), with the conclusion that nonnormality can seriously degrade the statistical performance of the Shewhart chart, but the EWMA and CUSUM charts can be designed to be robust. For example, with a large number of observations and a small smoothing parameter for the EWMA chart, a central limit theorem would ensure that the accumulation has approximately a normal distribution, which ensures robustness. Certainly, how small λ should be relies on the deviation of the actual measurement distribution from the normal distribution. Too small of smoothing parameters are usually not recommended because the corresponding procedure would not be sensitive to relatively large shifts.

As the CUSUM and EWMA charts have similar detection abilities and robustness demonstrated by the literature discussed, we choose only the EWMA chart for comparison. Denote $X^*_t = (X_t - \mu_0)/\sigma_0$, where μ_0 and σ_0 are the mean and standard deviation, respectively, which are known *a priori* or estimated from m_0 historical observations. The classical EWMA chart for detecting the mean change is defined as $w_t = (1-\lambda)w_{t-1} + \lambda X^*_t$. Reynolds and Stoumbos (2001) suggested using this chart combined with the following one-sided EWMA-type chart for monitoring the variance: $v_t = (1-\lambda)\max\{1, v_{t-1}\} + \lambda X^{*2}_t$. Hereafter, for abbreviation, we denote these two EWMA charts for the mean and variance as the EWM and EWV charts, respectively, and their combination as the CEW chart. Table 3 shows the ARL results of the NLE and CEW under the normal distribution. We consider two scenarios, $N(0,1)$ versus $N(\delta,1)$ for $\delta \ne 0$ and $N(0,1)$ versus $N(0,\delta^2)$ for $\delta \ne 1$, which correspond to the conventional univariate normal mean and variance monitoring problems, respectively. Three values of λ, 0.05, 0.1, and 0.2, were considered for both charts. Two m_0 values, 20000 and 200, are used, which correspond to the cases that F_0 is approximately known and the parameters are estimated. The control limits of the CEW chart with various combinations of m_0 and λ are obtained through simulations with the standard normal distribution. Because the CEW chart does not update the parameter estimates sequentially, we only report the zero-state OC ARLs here.

From this table, we observe that the CEW chart has superior efficiency for monitoring the mean change, as we would expect, because the parametric hypothesis is the correct one in this case. The NLE chart also offers quite satisfactory performance and the difference between NLE and EWMA is not very significant in detecting the small and moderate shifts. It should be pointed out that the superiority of EWMA becomes more significant when $m_0 = 200$ and δ is quite large, say, $\delta \ge 2$. The analogous phenomenon for univariate nonparametric charts has been mentioned in the literature, e.g., by Hackl and Ledolter (1991) and Zhou et al. (2009). The NLE, which is essentially based on ranks rather

TABLE 3. The Zero-State ARL Comparisons Between NLE and CEW Under the Normal Distribution

	$N(0,1)$ versus $N(\delta,1)$							$N(0,1)$ versus $N(0,\delta^2)$						
		NLE			CEW				NLE			CEW		
	δ	λ						δ	λ					
m_0		0.05	0.1	0.2	0.05	0.1	0.2		0.05	0.1	0.2	0.05	0.1	0.2
	0.00	369	370	370	370	372	369	1.00	370	370	371	370	368	371
	0.25	98.0	120	163	84.9	107	150	1.10	123	127	131	119	131	140
	0.50	36.1	37.7	49.2	29.3	33.0	43.9	1.20	57.0	58.4	61.4	54.6	60.8	66.8
	0.75	20.1	19.1	21.2	16.2	16.0	19.0	1.30	33.7	33.4	35.6	31.7	34.3	38.0
20000	1.00	14.1	12.2	11.9	11.0	10.3	10.7	1.40	23.0	22.4	23.1	21.1	22.6	24.9
	1.50	7.65	6.54	5.95	6.28	5.66	5.30	1.60	13.6	12.8	12.7	12.4	12.5	13.4
	2.00	4.57	4.01	3.67	4.04	3.69	3.44	1.80	9.47	8.82	8.60	8.64	8.51	8.76
	3.00	2.08	1.95	1.87	2.11	1.99	1.84	2.00	7.12	6.66	6.50	6.71	6.56	6.54
	4.00	1.30	1.26	1.24	1.41	1.32	1.25	3.00	3.30	3.19	3.10	3.28	3.15	3.06
	0.00	371	368	369	369	369	371	1.00	370	372	369	370	371	369
	0.25	152	192	243	112	139	177	1.10	212	215	220	132	139	151
	0.50	37.2	46.8	79.1	33.8	37.4	51.8	1.20	114	115	124	60.1	63.7	71.5
	0.75	20.4	19.4	23.8	18.1	17.6	20.7	1.30	64.2	65.0	72.7	34.4	36.7	40.4
200	1.00	14.3	12.5	12.5	12.3	11.1	11.6	1.40	41.4	41.2	44.7	23.1	23.8	26.0
	1.50	9.13	7.86	6.58	7.16	6.18	5.66	1.60	25.8	22.6	22.4	13.7	13.4	13.7
	2.00	6.73	5.79	4.68	4.67	4.10	3.66	1.80	19.4	16.4	14.9	9.51	9.15	9.21
	3.00	4.63	4.07	3.28	2.37	2.16	1.99	2.00	16.1	13.3	11.5	7.35	6.89	6.90
	4.00	4.02	3.54	2.89	1.52	1.39	1.30	3.00	10.1	8.27	6.49	3.53	3.32	3.18

than magnitudes, suffers from a similar drawback as those rank-based charts for univariate processes. That is, even though the shift is quite large, the ranks or signs of the observations may not be able to grow larger if m_0 is not large enough. It is interesting to see that, when m_0 is very large, the NLE even performs slightly better than the EWMA chart with the same value of λ in detecting very large shifts, say, $\delta \geq 3$. With respect to shifts in variance, the NLE chart performs better than CEW when $m_0 = 20000$ but the CEW is significantly superior to the NLE when $m_0 = 200$. We may conclude that, compared with the mean change, for detecting the dispersion change more efficiently, the NLE chart requires more IC observations before the change occurs.

Note that it may not be very fair to compare NLE and CEW using the zero-state OC ARL when m_0 is not large because the NLE is a self-starting one of which the performance may be severely contaminated if a change has occurred but the chart fails to signal quickly. However, if τ is large, the self-starting chart is capable of updating the IC distribution information with more IC observations, which in turn improves the detection ability. To appreciate this, Table 4 gives the ARL_δ values of the NLE chart with $\tau = 0, 50, 100, 200$ when $\lambda = 0.1$ and $m_0 = 200$. Naturally, the OC ARL will be affected by the number of reference samples gathered before a shift actually occurs. Yet the benefit is much more obvious in the case of detecting a small or large shift than in detecting a moderate shift.

Following the robustness analyses in Stoumbos and Reynolds (2000), besides the standard normal distribution, we consider the following distributions: (i) $t(3)$, the student t-distribution with three degrees of freedom; (ii) χ^2_3, the chi-square distribution with three degrees of freedom. For these two distributions, we standardize them so that they both have zero mean and unit variance. It is worth noting that we expect the EWV chart cannot easily be designed robust because the statistic v_t is not normal when the process observations X_t's are normally distributed. Thus, the CEW chart may not be relatively robust compared with the EWM chart. Therefore, the ARL_δ

TABLE 4. OC ARLs Values of the NLE Chart with Various Values of τ

δ	$N(0,1)$ versus $N(\delta,1)$ τ				δ	$N(0,1)$ versus $N(0,\delta^2)$ τ			
	0	50	100	200		0	50	100	200
0.00	368	367	362	366	1.00	372	367	364	365
0.25	192	182	169	160	1.10	215	195	187	173
0.50	46.8	44.4	41.8	39.8	1.20	115	98.1	89.1	80.7
0.75	19.4	19.6	19.1	18.9	1.30	65.0	52.0	47.5	43.0
1.00	12.5	12.3	12.2	12.2	1.40	41.2	32.1	30.0	28.1
1.50	7.86	6.78	6.63	6.61	1.60	22.6	17.5	16.6	15.7
2.00	5.79	4.34	4.26	4.21	1.80	16.4	12.2	11.5	11.1
3.00	4.07	2.47	2.39	2.34	2.00	13.3	9.41	8.99	8.58
4.00	3.54	1.94	1.89	1.83	3.00	8.27	5.09	4.83	4.59

results of EWM will also be presented for illustration. Two values of λ, 0.05 and 0.1, were considered for all three charts. As in Table 3, two m_0 values, 20000 and 200, are used. The control limits of the NLE and CEW charts with various combinations of m_0 and λ are the same as those in Table 3, while the control limits of the EWM chart are searched through simulations with the standard normal distribution. The simulation results with $\tau = 0$ for the distributions $t(3)$ and χ^2_3 are tabulated in Tables 5 and 6, respectively.

Just as in our intuitive analysis, the CEW usually has a very large bias in the IC ARL and, even when $\lambda = 0.05$, the degradation is still pronounced. Our other simulation results (not reported here) show that the IC ARL of CEW is close to the nominal one only when using $\lambda \le 0.001$ in the EWV chart. In contrast, the EWM chart is much more robust with $\lambda = 0.05$. In these situations, comparing the OC performance of CEW with the other two charts is meaningless. With similar IC ARL, the NLE is much better than the EWM in detecting small and moderate mean shifts when $m_0 = 200$, while the EWM has a certain advantage for the large shifts, as expected. For monitoring the shift in variance, the superiority of NLE over EWM is quite remarkable because the EWM is not sensitive to the variance change, as mentioned before. Note that Stoumbos and Reynolds (2000) also considered a combination of the EWM chart for the mean and an EWMA chart based on the absolute deviations from target for monitoring the variance. The absolute deviation chart may be a more robust alternative to the EWV chart for monitoring the variance. The performance comparison between this combination and NLE deserves future research.

Comparisons between NLE and Alternative Nonparametric Charts

Now we consider comparing NLE with some other nonparametric methods. Comparing the NLE procedure with alternative nonparametric methods turns out to be difficult due to the lack of an obvious comparable method. This is because most of the approaches in the literature are designed for monitoring locations. We only consider individual observations and comparable conclusions are similar for group observations. The EWMA chart with "standardized ranks" proposed by Hackl and Ledolter (1991) is a possible benchmark. Another alternative method is McDonald's (1990) CUSUM procedure based on "sequential ranks", but to avoid tuning of the reference parameter, its analogous EWMA procedure is considered. Hereafter, Hackl and Ledolter's chart is called HLE for short and McDonald's chart is called McE for short. In addition, we consider a natural modification of HLE, which is to replace the e.d.f. based on the reference sample by its sequential estimator. This modification is referred to as the self-starting HLE procedure (SHL) hereafter. To be specific, if the chart does not signal after the tth observation, then replace $F_{-m_0,0}(X_t)$ used in HLE by $F_{-m_0,t-1}(X_t)$. In these three charts and the NLE chart, we choose $\lambda = 0.1$. Note that the Shewhart chart for individual observations proposed by Chakraborti and Van de Wiel (2008) is a special case

TABLE 5. The Zero-State OC ARL Values of NLE, CEW, and EWM Under $t(3)$

	$t(3)/\sqrt{3}$ versus $t(3)/\sqrt{3}+\delta$							$t(3)/\sqrt{3}$ versus $\delta \cdot t(3)/\sqrt{3}$						
		NLE		CEW		EWM			NLE		CEW		EWM	
	δ	λ						δ	λ					
m_0		0.05	0.1	0.05	0.1	0.05	0.1		0.05	0.1	0.05	0.1	0.05	0.1
20000	0.00	372	371	127	108	365	272	1.00	370	369	128	108	362	266
	0.25	72.1	86.7	73.5	81.9	82.4	107	1.10	218	220	88.3	78.7	242	188
	0.50	28.4	26.8	28.6	34.5	27.0	32.0	1.20	127	132	65.6	59.0	175	137
	0.75	17.9	15.4	16.3	16.6	15.2	15.3	1.30	80.7	85.5	49.0	44.4	130	104
	1.00	13.3	10.9	11.1	10.4	10.6	9.67	1.40	56.7	60.3	38.1	35.6	103	80.0
	1.50	8.42	6.86	6.73	5.93	6.62	5.66	1.60	34.3	34.4	24.5	23.6	68.9	52.2
	2.00	6.04	4.89	4.44	3.93	4.90	4.10	1.80	24.2	23.2	17.4	16.5	49.9	38.0
	3.00	3.74	3.14	2.26	2.06	3.31	2.74	2.00	18.8	17.6	13.1	12.6	38.3	29.1
	4.00	2.70	2.35	1.43	1.29	2.56	2.12	3.00	9.21	8.10	5.78	5.49	16.4	12.2
200	0.00	370	371	131	113	408	300	1.00	370	369	128	115	401	303
	0.25	100	138	96.7	93.2	160	163	1.10	290	278	94.3	83.4	285	215
	0.50	25.5	26.2	49.7	55.5	48.4	58.1	1.20	206	207	73.9	63.7	213	162
	0.75	15.7	13.8	25.8	29.0	26.3	30.7	1.30	142	146	55.4	51.3	160	122
	1.00	11.8	10.1	16.5	19.1	18.2	16.2	1.40	95.3	100	46.6	39.9	136	99.3
	1.50	8.16	7.05	9.40	11.5	9.31	10.3	1.60	50.3	52.9	28.9	27.8	90.1	64.6
	2.00	6.53	5.66	6.84	5.63	6.30	7.40	1.80	33.3	32.5	21.2	20.0	67.8	45.4
	3.00	5.01	4.40	2.34	2.92	3.36	3.93	2.00	25.8	23.6	15.9	14.2	51.6	38.4
	4.00	4.42	3.88	1.47	2.56	2.56	2.15	3.00	14.3	11.8	6.88	6.43	19.7	14.3

of the HLE chart with $\lambda = 1$, while the change-point scheme proposed by Zhou et al. (2009) is an analog of the SHL chart. Their difference lies mainly in how to use the Mann–Whitney statistic to construct the control scheme rather than in the test itself. Hence, we believe that the comparison of these four EWMA charts suffices to show the effectiveness of our proposed scheme. Table 7 lists the abbreviations and brief descriptions of the nonparametric charts utilized for performance comparisons.

In order to assess the overall performance of a chart among all the charts considered across a range of shift sizes, besides OC ARLs, we also compute their relative mean index (RMI) values. The RMI index of a control chart is suggested by Han and Tsung (2006) and is defined as

$$\mathrm{RMI} = \frac{1}{N}\sum_{l=1}^{N}\frac{\mathrm{ARL}_{\delta_l} - \mathrm{MARL}_{\delta_l}}{\mathrm{MARL}_{\delta_l}},$$

where N is the total number of shifts considered, ARL_{δ_l} is the OC ARL of the given control chart when detecting shift δ_l, and MARL_{δ_l} is the smallest OC ARL among all OC ARL values of the charts considered when detecting shift δ_l. So $(\mathrm{ARL}_{\delta_l} - \mathrm{MARL}_{\delta_l})/\mathrm{MARL}_{\delta_l}$ can be considered as a relative efficiency measure of the given control chart, compared with the best chart, when detecting shift δ_l, and RMI is the average of all such relative efficiency values. By this index, a control chart with a smaller RMI value is considered better on the whole. For various IC and OC distributions, all simulated OC ARLs are illustrated with graphs in the log scale, where the ARLs are plotted against the shift magnitude, δ, which is selected with different ranges in different comparison scenarios. In the legend of each plot, the numbers in parentheses are the RMI values evaluated with $N = 20$ magnitudes of shifts across the considered range of δ. The solid, dashed, dotted, and dashed-dotted curves represent the OC ARLs of the NLE, HLE, McE, and SHL charts, respectively.

We first consider the following two comparison scenarios under the normal distribution: (I) $N(0,1)$ versus $N(\delta,1)$ for $\delta \neq 0$ and (II) $N(0,1)$ versus

TABLE 6. The Zero-State OC ARL Values of NLE, CEW, and EWM Under χ^2_3

	$(\chi^2_3-3)/\sqrt{6}$ versus $(\chi^2_3-3)/\sqrt{6}+\delta$							$(\chi^2_3-3)/\sqrt{6}$ versus $\delta\cdot(\chi^2_3-3)/\sqrt{6}$						
		NLE		CEW		EWM			NLE		CEW		EWM	
	δ			λ				δ			λ			
m_0		0.05	0.1	0.05	0.1	0.05	0.1		0.05	0.1	0.05	0.1	0.05	0.1
	0.00	373	370	120	101	373	297	1.00	374	372	118	100	366	296
	0.25	54.4	88.7	65.0	61.7	72.0	75.3	1.10	23.6	23.4	72.9	66.6	224	193
	0.50	30.7	26.8	29.4	30.9	27.7	29.1	1.20	11.0	10.9	48.4	46.9	153	131
	0.75	22.7	18.4	17.1	17.0	16.0	15.6	1.30	7.49	7.36	34.4	34.7	109	92.8
20000	1.00	17.9	14.4	11.8	11.0	11.1	10.3	1.40	5.69	5.67	25.8	26.1	82.2	69.5
	1.50	12.3	9.82	7.03	6.23	6.95	6.02	1.60	4.06	4.06	16.5	16.9	53.5	42.2
	2.00	8.91	7.12	4.65	4.17	5.09	4.28	1.80	3.35	3.30	11.7	11.7	37.9	29.0
	3.00	5.11	4.22	2.32	2.16	3.42	2.81	2.00	2.92	2.92	9.03	9.01	28.8	21.6
	4.00	3.22	2.76	1.48	1.39	2.65	2.17	3.00	2.05	2.03	3.99	3.80	12.1	8.62
	0.00	373	366	122	105	421	380	1.00	370	373	121	105	425	381
	0.25	57.1	191	75.4	68.0	101	97.8	1.10	117	128	75.9	68.5	255	236
	0.50	22.9	22.9	34.0	34.9	31.8	34.1	1.20	46.2	49.8	51.6	48.6	173	151
	0.75	16.9	14.9	18.4	18.3	17.2	16.9	1.30	29.6	27.9	36.4	35.7	125	105
200	1.00	13.9	11.9	12.3	11.6	11.6	10.8	1.40	22.9	19.9	28.1	27.1	95.1	77.5
	1.50	10.3	8.85	7.26	6.36	7.08	6.11	1.60	17.0	14.2	17.9	17.7	60.9	46.8
	2.00	8.32	7.15	4.93	4.26	5.17	4.30	1.80	14.1	11.7	12.8	12.5	44.3	31.9
	3.00	5.94	5.17	2.51	2.28	3.44	2.80	2.00	12.4	10.2	9.75	9.40	33.3	23.5
	4.00	4.77	4.17	1.57	1.44	2.66	2.13	3.00	8.92	7.47	4.44	4.09	13.8	9.49

$N(0,\delta^2)$ for $\delta > 1$. The cases that $m_0 = 50, 200$ and $\tau = 50, 150$ were considered. The simulation results are shown in Figures 2 and 3. We observe the following results. First, the NLE chart is more effective than the other three charts in detecting moderate and large shifts in the process mean. The superiority of NLE becomes more significant as δ becomes larger while the OC ARLs of the other three charts hardly change when $\delta > 3$. The control charts based on linear transformation of ranks, such as HLE, McE, and SHL charts, share this drawback. Even though the shift is quite large, the ranks of the observations may not be able to grow larger because the reference sample for calculating the ranks is usually not sufficiently large. The NLE chart, which derives from the nonparametric likelihood ratio test, is a nonlinear function of ranks and thus overcomes this drawback to some degree. Second, for small shifts, the other

TABLE 7. The Abbreviations and Descriptions of the Nonparametric Charts Utilized for Performance Comparisons. The generic notation R_i, R_i^*, and w_t are used in each chart, which should not cause any confusion

HLE: Define the standardized rank as $R_i = 2(m_0+1)^{-1}[R_i^* - (m_0+2)/2]$, where R_i^* is the rank of X_i with respect to the historical sample. The HLE charting statistic is $w_t = (1-\lambda)w_{t-1} + \lambda R_t$ with $w_0 = 0$.

SHL: Define the standardized rank as $R_i = 2(m_0+i)^{-1}[R_i^* - (m_0+i+1)/2]$ where R_i^* is the rank of X_i with respect to the aligned observations of the historical and $i-1$ Phase II observations. Say, $R_i = 1 + \sum_{j=-m_0+1}^{i-1} I_{\{X_j \le X_i\}}$. The SHL charting statistic is $w_t = (1-\lambda)w_{t-1} + \lambda R_t$ with $w_0 = 0$.

McE: Define the sequential rank R_i of an observation X_i as $R_i = 1 + \sum_{j=1}^{i-1} I_{\{X_j \le X_i\}}$. The McE charting statistic is $w_t = (1-\lambda)w_{t-1} + \lambda(R_t/(t+1) - 0.5)$ with $w_0 = 0$.

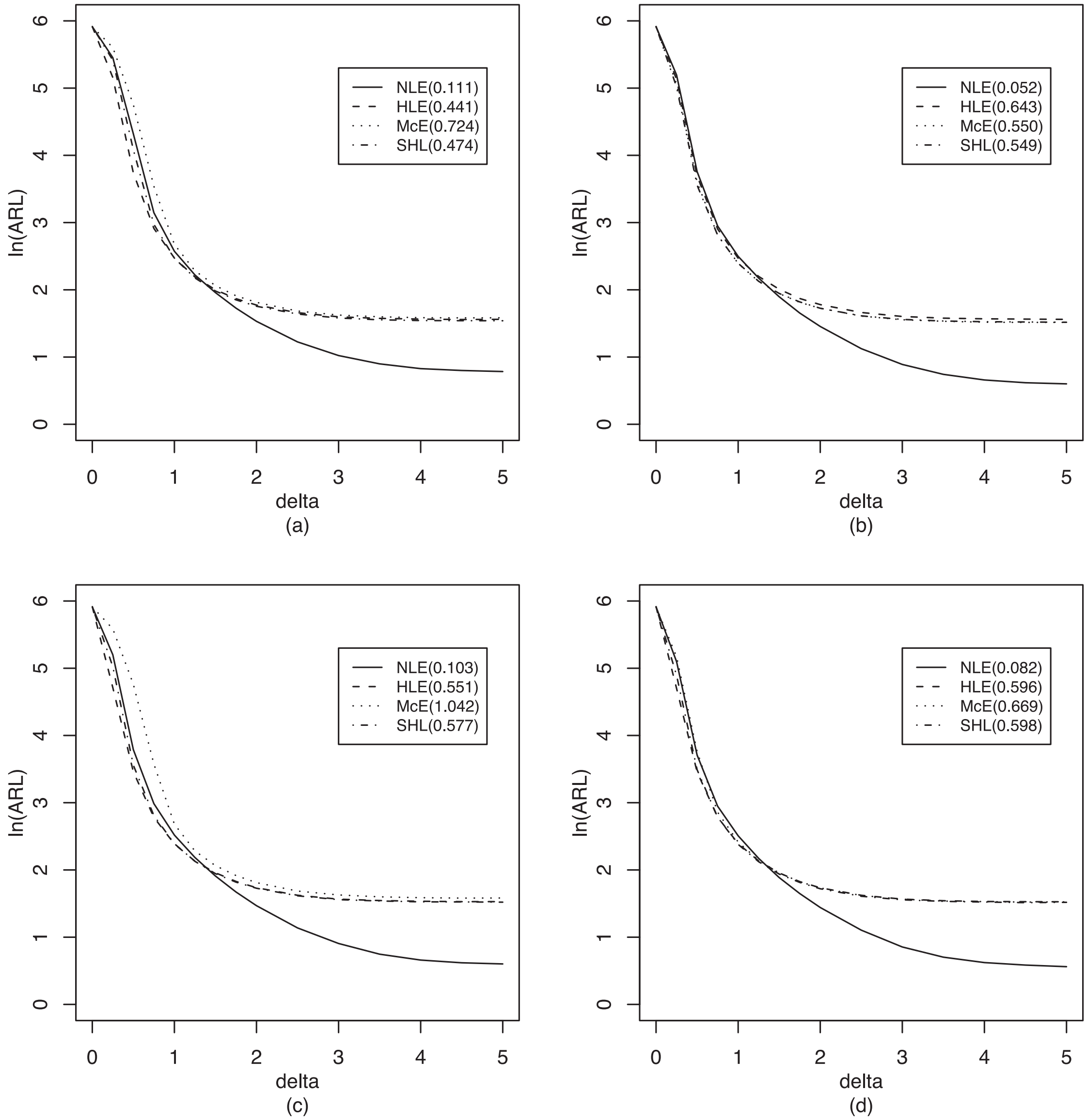

FIGURE 2. OC ARL Comparison of the NLE, HLE, McE, and SHL Charts for Monitoring $N(0, 1)$ Versus $N(\delta, 1)$ When: (a) $m_0 = 50$, $\tau = 50$; (b) $m_0 = 50$, $\tau = 150$; (c) $m_0 = 200$, $\tau = 50$; (d) $m_0 = 200$, $\tau = 150$.

three EWMA charts generally offer faster detection than NLE does, although the difference is relatively small, especially when $\tau = 150$. This is because the NLE chart is an omnibus chart, whereas the others are designed to be sensitive to location shifts. Third, the NLE chart outperforms the other charts in detecting variance shifts by quite a large margin, which demonstrates the fact that it is more sensitive to the scale compared with the conventional rank tests. Note that here we only report the performance comparison in detecting the increase in variance. In fact, our additional simulation results (not reported here but available from the authors) show that the NLE chart is quite effective in detecting the decrease in variance as well. Fourth, in terms of the RMI index, NLE performs the best overall. Its superiority becomes more remarkable as m_0 and τ increase due to making full use of information from the historical and new observations. It is worth mentioning that SHL performs a little better than HLE when τ is large because the "masking" effect (Hawkins and Olwell (1998)) is diminished in such a situation, which

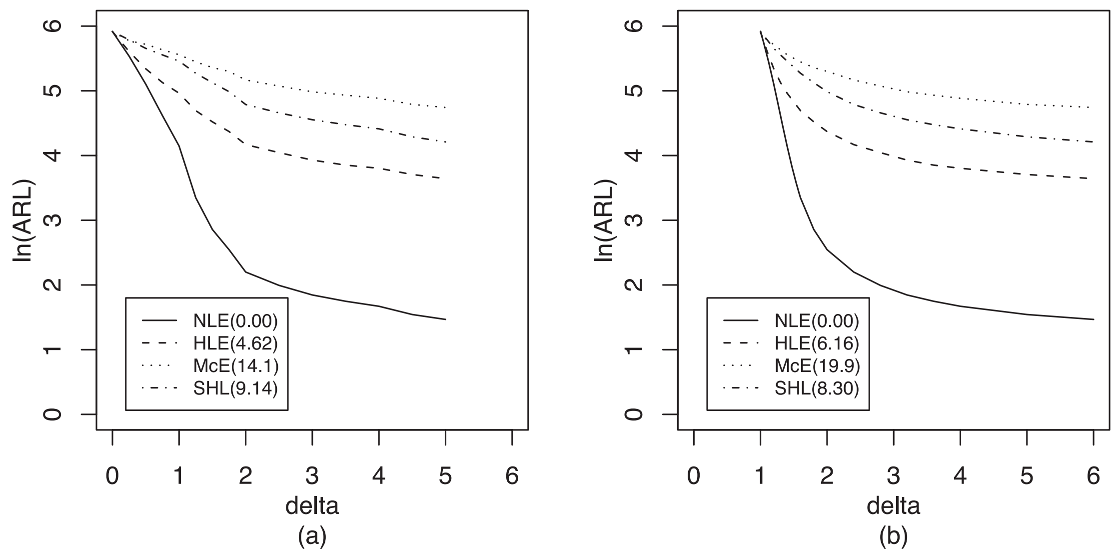

FIGURE 3. OC ARL Comparison of the NLE, HLE, McE, and SHL Charts for Monitoring $N(0, 1)$ Versus $N(0, \delta^2)$ When: (a) $m_0 = 50$, $\tau = 50$; (b) $m_0 = 200$, $\tau = 50$.

is consistent with the findings in Quesenberry (1995) and Hawkins et al. (2003) about univariate normal processes.

Figure 4 shows the ARL_δ curves for monitoring the mean and variance change when the underlying process distributions are $t(3)$ and χ^2_3. The shift models considered in this figure are the same as those in Tables 5 and 6. Because a similar conclusion holds for other cases, here we only present the results when $m_0 = 200$ and $\tau = 50$ for illustration. In both figures, the ARL_δ improvement in NLE over the other three charts for detecting the change in scale is tremendous, as we would expect. It has at least comparable performance when the shift comes only from the mean. This demonstrates that the NLE chart offers robust protection against variation in various under lying distributions. Some additional simulation results (not reported here; available from the authors) also show that the NLE chart is capable of detecting other distributional changes, such as the shifts in shape.

Diagnostic Performance Analysis

Finally, we investigate the performance of the proposed approach in estimating the change point and the diagnostic ability of the tests T_W and T_A after the NLE chart has signalled. Ten thousand independent series were generated in the simulations. Note that any series for which no signal was trigged was discarded. Again, the process change point was simulated at $\tau = 50$ and $m_0 = 200$. To quantify the diagnostic precision of the estimator $\widehat{\tau}$ in Equation (10), in addition to calculating the median (MED) of the change-point estimates, we also tabulate the probabilities, $\Pr(|\widehat{\tau} - \tau| = 0)$, $\Pr(|\widehat{\tau} - \tau| \le 1)$, and $\Pr(|\widehat{\tau} - \tau| \le 2)$ (denoted as P_0, P_1, and P_2, respectively) in Table 8. Also, columns 7–9 of Table 8 give, respectively, estimates of the probabilities $\Pr(T_W \text{ issignificantalone})$, $\Pr(T_A \text{ issignificantalone})$, and $\Pr(\text{bothtestsaresignificant})$, denoted as P_{T_W}, P_{T_A}, and P_{Both}, for shifts in the mean alone, in the dispersion alone, and in both. The significant level was fixed at 0.01 for both tests. Four scenarios were considered: (i) $N(0,1)$ versus $N(\delta,1)$; (ii) $N(0,1)$ versus $N(0,\delta^2)$; (iii) $t(3)/\sqrt{3}$ versus $t(3)/\sqrt{3}+\delta$; (iv) $t(3)/\sqrt{3}$ versus $\delta \cdot t(3)/\sqrt{3}$. Note that, for a given entry with relative frequency $\widehat{\pi}$, its standard error can be computed by the formula $\sqrt{\widehat{\pi}(1-\widehat{\pi})/10000}$.

Table 8 shows that the proposed change-point estimator performs well from the viewpoint of the median for any shift size and $\widehat{\tau}$ has better precision as the magnitude of the shift increases. We can also see that $\widehat{\tau}$ performs much better for monitoring mean changes than for dispersion changes in terms of the accurate probabilities. With respect to the combination of two diagnostic tests, it is likely that the T_W alone will be significant when there is a small shift in the mean, and both tests will be significant when there is a large shift in the mean. It is likely that

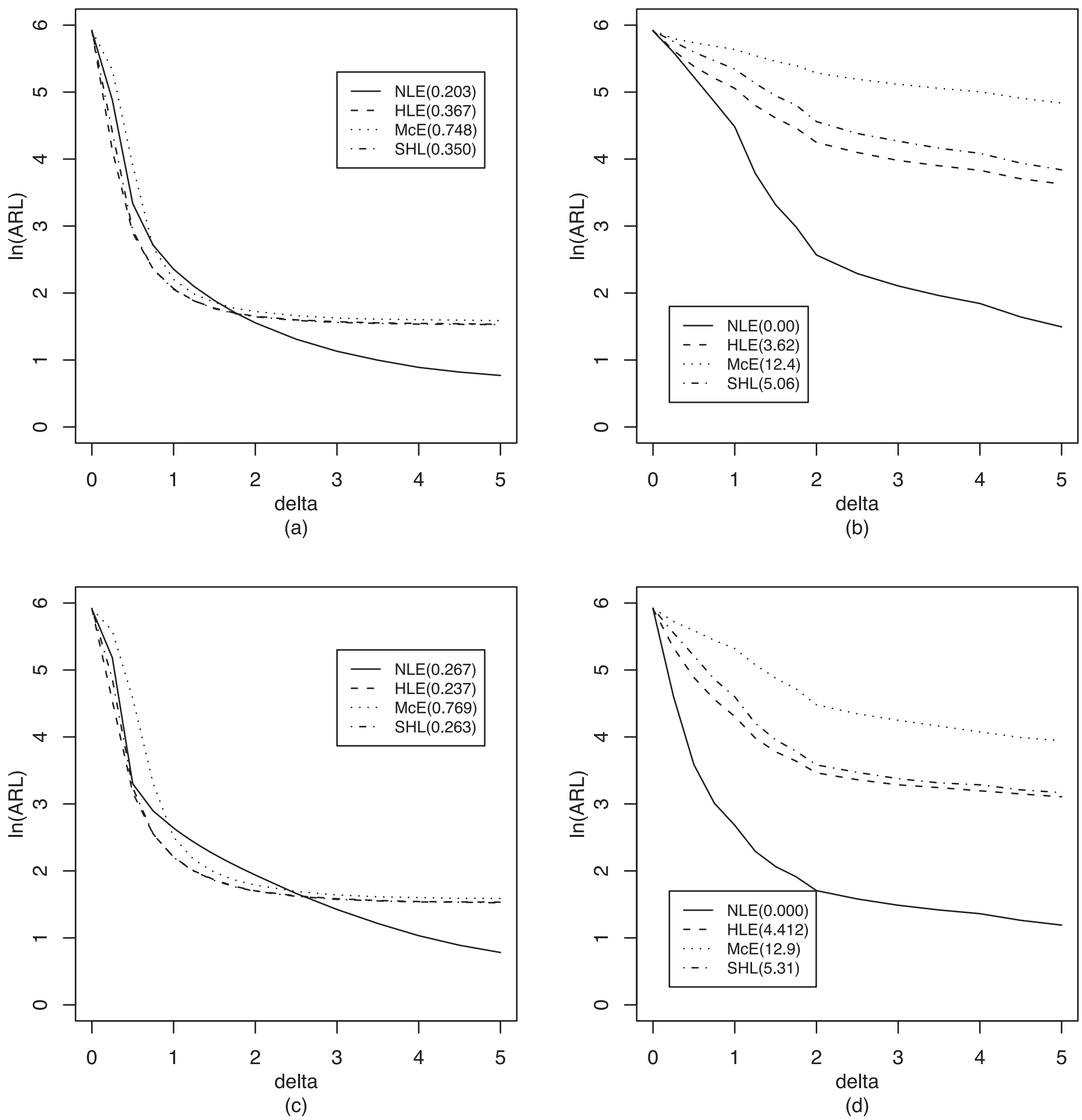

FIGURE 4. ARL Comparison of the NLE, HLE, McE, and SHL Charts for Monitoring: (a) $t(3)/\sqrt{3}$ Versus $t(3)/\sqrt{3}+\delta$; (b) $t(3)/\sqrt{3}$ Versus $\delta \cdot t(3)/\sqrt{3}$; (c) $(\chi_3^2-3)/\sqrt{6}$ Versus $(\chi_3^2-3)/\sqrt{6}+\delta$; (d) $(\chi_3^2-3)/\sqrt{6}$ Versus $\delta \cdot (\chi_3^2-3)/\sqrt{6}$ When $m_0 = 200$, $\tau = 50$.

rolling, soaking, assembly, cleaning, aging, and classifying. The quality of unfinished AEC products that are called capacitor elements in terms of appearance condition and functional performance will be inspected by sampling after each stage. In each stage, some important characteristics in the specification of an AEC, such as the capacitance and loss tangent (or equivalently dissipation factor), are automatically calibrated by an electronic device at some given measuring voltage, frequency, and temperature.

To illustrate, we consider the monitoring of the capacitance values (X_t) at the aging stage. The dataset comprises 200 observations. Figure 5(a) shows the time-series plots of the raw data. Among them, the last 30 observations are suspected as inferior products based on engineering knowledge. So we use the first 170 observations as the historical sample (i.e., $m_0 = 170$) and the others for test. A calibration sample of this size may be smaller than ideal to determine fully the IC distribution but it suffices to use

TABLE 8. Diagnostic Results of the Change-Point Estimate $\widehat{\tau}$ in (10) and T_W and T_A Tests in the Cases When (i) $N(0, 1)$ Versus $N(\delta, 1)$; (ii) $N(0, 1)$ Versus $N(1, \delta^2)$; (iii) $t(3)/\sqrt{3}$ Versus $t(3)/\sqrt{3} + \delta$; (iv) $t(3)/\sqrt{3}$ Versus $\delta \cdot t(3)/\sqrt{3}$

δ	MED	P_0	P_1	P_2	P_{T_W}	P_{T_A}	P_{both}	
	0.50	51	0.076	0.166	0.235	0.783	0.048	0.043
	0.75	50	0.144	0.287	0.384	0.790	0.047	0.074
	1.25	50	0.221	0.404	0.518	0.742	0.061	0.133
(i)	1.50	50	0.307	0.513	0.629	0.639	0.084	0.224
	1.75	50	0.396	0.609	0.724	0.512	0.109	0.332
	2.00	50	0.469	0.681	0.778	0.368	0.146	0.443
	2.50	50	0.538	0.741	0.820	0.233	0.197	0.526
	1.50	52	0.066	0.156	0.232	0.106	0.613	0.145
	1.75	51	0.095	0.202	0.289	0.081	0.630	0.163
	2.00	50	0.129	0.264	0.360	0.062	0.667	0.161
(ii)	2.25	50	0.194	0.357	0.475	0.037	0.689	0.181
	2.50	50	0.245	0.439	0.552	0.027	0.723	0.171
	3.00	50	0.292	0.493	0.612	0.020	0.736	0.171
	4.00	50	0.311	0.523	0.637	0.016	0.749	0.167
	0.50	50	0.123	0.244	0.331	0.820	0.036	0.115
	0.75	50	0.241	0.421	0.530	0.838	0.026	0.121
	1.25	50	0.364	0.571	0.687	0.803	0.027	0.157
(iii)	1.50	50	0.471	0.670	0.777	0.728	0.029	0.231
	1.75	50	0.571	0.762	0.846	0.612	0.039	0.334
	2.00	50	0.635	0.811	0.877	0.448	0.053	0.484
	2.50	50	0.695	0.843	0.897	0.291	0.082	0.610
	1.50	54	0.031	0.078	0.118	0.144	0.558	0.166
	1.75	52	0.055	0.121	0.178	0.122	0.596	0.173
	2.00	51	0.072	0.164	0.238	0.110	0.611	0.187
(iv)	2.25	51	0.126	0.252	0.348	0.069	0.652	0.203
	2.50	50	0.159	0.311	0.420	0.058	0.663	0.212
	3.00	50	0.202	0.374	0.487	0.042	0.669	0.228
	4.00	50	0.226	0.412	0.532	0.037	0.688	0.222

the T_A alone will be significant when there is a shift in the dispersion. Actually, this finding is consistent with that of using the combination of two EWMA charts in Reynolds and Stoumbos (2001). By comparing the results given in Table 3 of Reynolds and Stoumbos (2001), the main conclusion is that the use of nonparametric post-diagnostic tests is at least as reliable as the combination of two EWMA charts in identifying the type of parameter change that has occurred. Our additional simulation results (not reported here) also indicate that the same conclusion could be drawn in the case that both the mean and variance change at the same time.

A Real-Data Application

In this section, we demonstrate the proposed methodology by applying it to a real dataset from an aluminium electrolytic capacitor manufacturing process. The aim of an aluminium electrolytic capacitor (AEC) process is to transform the raw materials (anode aluminum foil, cathode aluminum foil, guiding pin, electrolyte sheet, plastic cover, aluminum shell, and plastic tube) into AECs with specific specifications. The whole manufacturing process, which is a typical multistage process (c.f., Shi (2007)), includes a sequence of operations, such as clenching,

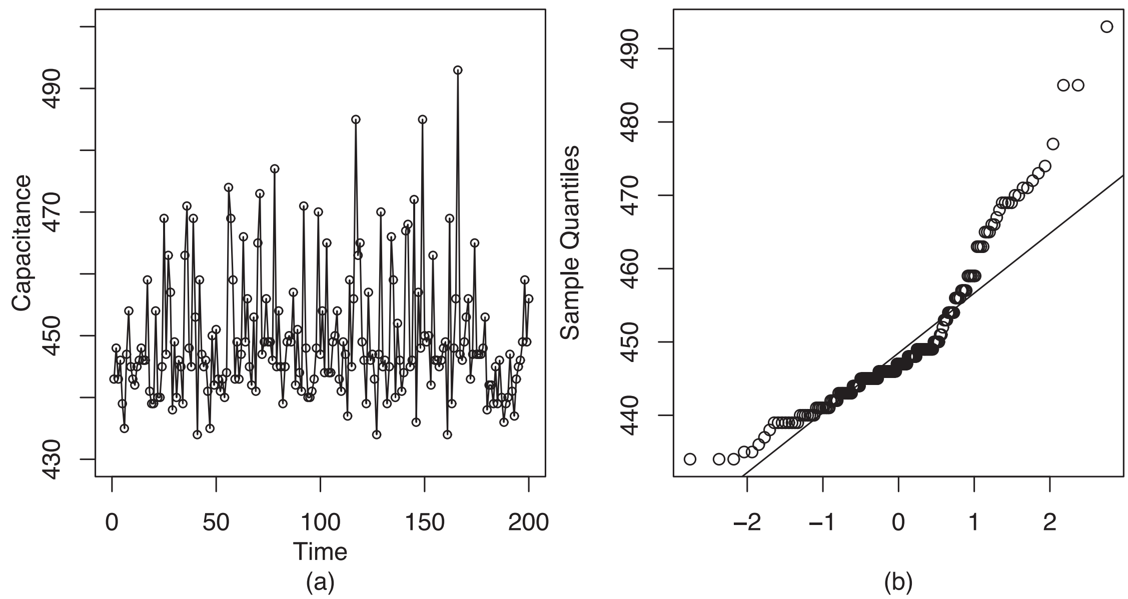

FIGURE 5. (a) The Time Series Plot of the Aluminium Electrolytic Capacitors Data. (b) The Normal Q-Q Plot for the Capacitance Observations.

our proposed NLE chart because it is a distribution-free scheme. We use the standard X and MR control charts (Montgomery (2005)) to see whether these observations were taken from a stable process. Neither of the two charts triggers a signal with the false-alarm rate 0.01. The normality assumption on the distribution may be poor, as suggested by the quantile-quantile (Q-Q) plot for the 170 historical observations in Figure 5(b). In fact, a one-sample Kolmogorov–Smirnov test for normality is highly significant (p-value is smaller than 0.0001). All these checkings suggest that the normality assumption on

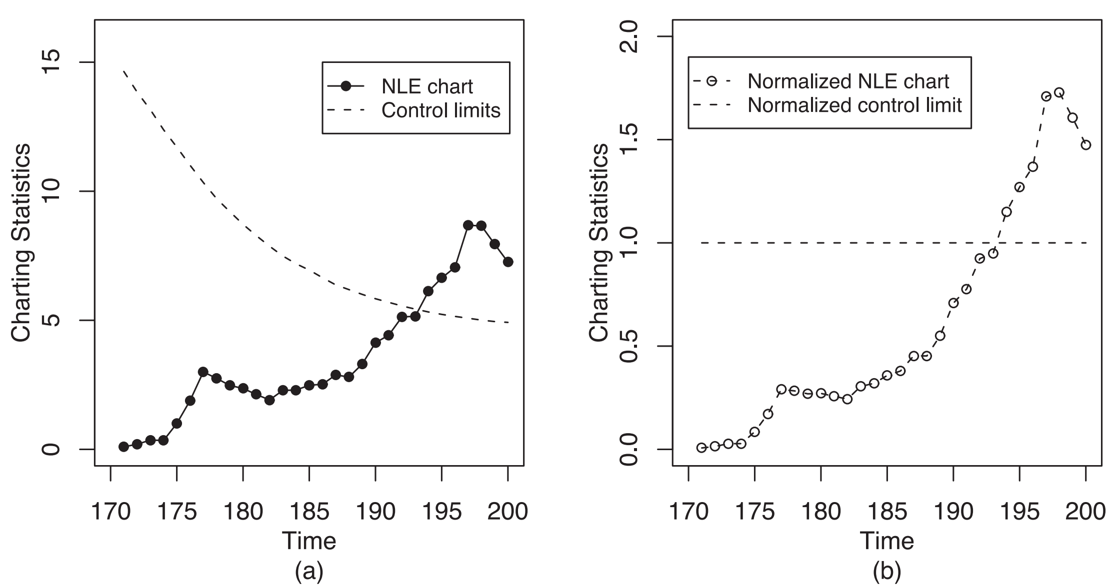

FIGURE 6. (a) The NLE Control Chart along with the Control Limits (Dashed Line) for Monitoring the Aluminium Electrolytic Capacitor Process. (b) The Normalized NLE Control Chart along with the Normalized Control Limit One for Monitoring the Aluminium Electrolytic Capacitor Process.

F_0 is not valid and, thus, we would expect that the nonparametric scheme should be more robust and powerful than normal-based schemes for this dataset.

Now we are ready to construct the proposed NLE chart for Phase II analysis. Its IC ARL is fixed at 370 and λ is chosen to be 0.1. Note that $m_0 = 170$ is not contained in Table 2 and, thus, the control limits are obtained from Equation (8) through additional simulations (it costs about 4 minutes to find the control limits based on 250,000 replications). Figure 6(a) shows the resulting NLE chart (solid curve connecting the dots) along with its dynamic control limits (the dashed line). The corresponding normalized NLE chart (dashed curve connecting circles) and its constant control limit are presented in Figure 6(b). The charting statistics and the diagnostic statistics $Z_A(t, k)$ are tabulated in Table 9. From the plot and table, it can be seen that the NLE chart passes the control limit at around the 194th observation and it remains above the control limit for the remaining observations. This excursion suggests that a marked step change has occurred. Then by looking at the values of $Z_A(t, 24)$ for $t = 0, 1, \cdots, 23$, we find that its maximum occurs at $t = 9$ with $Z_A(9, 24) = 48.244$. In addition, by computing the test statistics given T_W and T_A in Equations (11) and (12), respectively, we can obtain the corresponding p-values of 2×10^{-4} and 0.03, which indicate that there has been a shift in the location.

TABLE 9. Data and Statistics for the Aluminium Electrolytic Capacitor Dataset

t	X_t	$\tilde{Z}_t$	L_t	$\tilde{Z}_t/L_t$	$Z_A(t,k)$
0					8.122
1	456	0.098	14.639	0.007	18.589
2	443	0.198	13.842	0.014	17.306
3	447	0.358	13.159	0.027	18.055
4	465	0.345	12.382	0.028	27.551
5	447	1.001	11.709	0.085	28.524
6	447	1.889	11.006	0.172	29.801
7	447	3.000	10.339	0.290	31.301
8	448	2.751	9.715	0.283	33.756
9	453	2.476	9.209	0.269	48.244
10	438	2.360	8.717	0.271	41.123
11	442	2.127	8.280	0.257	37.788
12	442	1.915	7.871	0.243	33.811
13	439	2.283	7.492	0.305	28.963
14	445	2.297	7.191	0.319	27.327
15	439	2.483	6.945	0.358	22.382
16	446	2.522	6.650	0.379	22.749
17	440	2.885	6.372	0.453	19.244
18	436	2.800	6.188	0.452	13.205
19	439	3.306	6.004	0.551	8.643
20	440	4.131	5.835	0.708	5.425
21	447	4.423	5.695	0.777	7.815
22	441	5.132	5.555	0.924	4.526
23	437	5.154	5.433	0.949	0.596
24	443	6.121	5.322	1.150	1.292
25	445	6.640	5.229	1.270	0.047
26	446	7.052	5.151	1.369	
27	449	8.680	5.080	1.709	
28	459	8.658	5.007	1.729	
29	449	7.947	4.951	1.605	
30	456	7.256	4.919	1.475	

Concluding Remarks

In this paper, we propose a univariate distribution-free control chart. This chart integrates Zhang's (2002) powerful goodness-of-fit test and EWMA process monitoring. It can be easily implemented when the underlying process distribution is unknown and, thus, a lengthy data-gathering step can be avoided. The proposed scheme is fast in computation, convenient to use, and efficient in detecting potential shifts in location or scale. Numerical results show that it is not only sensitive to shifts in location or mean in the process, but also remarkably effective in detecting changes in the scale and shape at which the conventional rank-based control charts are inefficient. Additional numerical studies (not reported in the paper) show that it is effective in detecting certain drift changes as well.

Hawkins et al.'s (2003) change-point scheme for on-line monitoring can also be seen as a self-starting method. Zhou et al. (2009) and Hawkins and Deng (2010) extended this strategy to the nonparametric setting by utilizing the two-sample Mann–Whitney test statistics. In an ongoing effort, we are developing a control scheme that integrates sequential change-point detection and the two-sample GOF test proposed by Zhang (2006), which might be expected to be more robust in detecting various magnitudes of shifts and in further alleviating the masking effect at a certain expense of computational effort.

Acknowledgments

The authors thank the editor and two anonymous referees for their many helpful comments that have resulted in significant improvements in the article.

The authors are also grateful to HKUST Quality Lab for providing the real data and context of the example. This work was completed when Zou was a Postdoctoral Fellow at the Hong Kong University of Science and Technology, whose hospitality is appreciated and acknowledged. This research was supported by the NNSF of China Grants 10771107 and RGC Competitive Earmarked Research Grants 620508 and 620707.

References

Albers, W. and Kallenberg, W. C. M. (2004). "Empirical Nonparametric Control Charts: Estimation Effects and Corrections". *Journal of Applied Statistics* 31, pp. 345–360.

Anderson, T. W. (1962). "On the Distribution of the Two-Sample Cramér-von Mises Criterion". *The Annals of Mathematical Statistics* 33, pp. 1148–1159.

Bakir, S. T. (2004). "A Distribution-Free Shewhart Quality Control Chart Based on Signed-Ranks". *Quality Engineering* 16, pp. 611–623.

Bakir, S. T. (2006). "Distribution-Free Quality Control Charts Based on Signed-Rank-Like Statistics". *Communications in Statistics: Theory and Methods* 35, pp. 743–757.

Bakir S, T. and Reynolds, Jr., M. R. (1979). "A Nonparametric Procedure for Process Control Based on Within-Group Ranking". *Technometrics* 21, pp. 175–183.

Borror, C. M.; Montgomery, D. C.; and Runger, G. C. (1999). "Robustness of EWMA Control Chart to Non-Normality". *Journal of Quality Technology* 31, pp. 309–316.

Capizzi, G. and Masarotto, G. (2003). "An Adaptive Exponentially Weighted Moving Average Control Chart". *Technometrics* 45, pp. 199–207.

Chakraborti, S.; Eryilmaz, S.; and Human, S. W. (2009). "A Phase II Nonparametric Control Chart Based on Precedence Statistics with Runs-Type Signaling Rules". *Computational Statistics and Data Analysis* 53, pp. 1054–1065.

Chakraborti, S.; van der Laan, P.; and van de Wiel, M. A. (2004). "A Class of Distribution-Free Control Charts". *Journal of the Royal Statistical Society, Series C* 53, pp. 443–462.

Chakraborti, S.; van der Laan, P.; and Bakir, S. T. (2001). "Nonparametric Control Charts: An Overview and Some Results". *Journal of Quality Technology* 33, pp. 304–315.

Chakraborti, S. and van de Wiel, M. A. (2008). "A Nonparametric Control Chart Based on the Mann–Whitney Statistic". *IMS Collections. Beyond Parametrics in Interdisciplinary Research: Festschrift in Honor of Professor Pranab K. Sen* 1, pp. 156–172.

Chen, G.; Cheng, S. W.; and Xie, H. (2001). "Monitoring Process Mean and Variability with One EWMA Chart". *Journal of Quality Technology* 33, pp. 223–233.

Conover, W. J. (1999). *Practical Nonparametric Statistics*, 3rd edition. New York, NY: Wiley.

Conover, W. J.; Johnson, M. E.; and Johnson, M. M. (1981). "A Comparative Study of Tests for Homogeneity of Variances, with Applications to the Outer Continental Shelf Bidding Data". *Technometrics* 23, pp. 351–361.

Csorgo, M. and Horvath, L. (1998). *Limit Theorems in Change-Point Analysis*. New York, NY: John Wiley.

Einmahl, J. H. J. and McKeague, I. W. (2003). "Empirical Likelihood Based Hypothesis Testing". *Bernoulli* 9, pp. 267–290.

Fligner, M. A. and Killeen, T. J. (1976). "Distribution-Free Two-Sample Test for Scale". *Journal of the American Statistical Association* 71, pp. 210–213.

Hackl, P. and Ledolter, J. (1991). "A Control Chart Based on Ranks". *Journal of Quality Technology* 23, pp. 117–124.

Han D. and Tsung, F. (2006). "A Reference-Free Cuscore Chart for Dynamic Mean Change Detection and a Unified Framework for Charting Performance Comparison". *Journal of the American Statistical Association* 101, pp. 368–386.

Han, D.; Tsung, F.; Hu, X.; and Wang, K. (2007). "CUSUM and EWMA Multi-Charts for Detecting a Range of Mean Shifts". *Statistica Sinica* 17, pp. 1139–1164.

Hawkins, D. M. (1987). "Self-Starting CUSUM Charts for Location and Scale". *The Statistician* 36, pp. 299–316.

Hawkins, D. M. and Deng, Q. (2010). "A Nonparametric Change Point Control Chart". *Journal of Quality Technology* 42, pp. 000–000.

Hawkins, D. M. and Olwell, D. H. (1998). *Cumulative Sum Charts and Charting for Quality Improvement*. New York, NY: Springer-Verlag.

Hawkins, D. M.; Qiu, P.; and Kang, C. W. (2003). "The Changepoint Model for Statistical Process Control". *Journal of Quality Technology* 35, pp. 355–366.

Hawkins, D. M. and Zamba, K. D. (2005). "Statistical Process Control for Shifts in Mean or Variance Using a Change Point Formulation". *Technometrics* 47, pp. 164–173.

Jensen, W. A.; Jones-Farmer, L. A.; Champ, C. W.; and Woodall, W. H. (2006). "Effects of Parameter Estimation on Control Chart Properties: A Literature Review". *Journal of Quality Technology* 38, pp. 349–364.

Jones-Farmer, L. A. (2002). "The Statistical Design of EWMA Control Charts with Estimated Parameters". *Journal of Quality Technology* 34, pp. 277–288.

Jones-Farmer, L. A.; Jordan, V.; and Champ, C. W. (2009). "Distribution-Free Phase I Control Charts for Subgroup Location". *Journal of Quality Technology* 41, pp. 304–316.

Lai, T. L. (1995). "Sequential Changepoint Detection in Quality Control and Dynamical Systems". *Journal of the Royal Statistical Society, Series B* 57, pp. 613–658.

Liu, R. (1995). "Control Charts for Multivariate Processes". *Journal of the American Statistical Association* 90, pp. 1380–1387.

Lucas, J. M. and Saccucci, M. S. (1990). "Exponentially Weighted Moving Average Control Schemes: Properties and Enhancements". *Technometrics* 32, pp. 1–29.

McDonald, D. (1990). "A CUSUM Procedure Based on Sequential Ranks". *Naval Logistic Research* 37, pp. 627–646.

Montgomery, D. C. (2005). *Introduction to Statistical Quality Control*, 5th edition. New York, NY: John Wiley & Sons.

Pignatiello, Jr., J. J. and Samuel, T. R. (2001). "Estimation of the Change Point of a Normal Process Mean in SPC Applications," *Journal of Quality Technology* 33, pp. 82–95.

Qiu, P. (2008). "Distribution-Free Multivariate Process Control Based on Log-Linear Modeling". *IIE Transactions* 40, pp. 664–677.

Qiu, P. and Hawkins, D. M. (2001). "A Rank-Based Multivariate CUSUM Procedure". *Technometrics* 43, pp. 120–132.

Quesenberry, C. P. (1991). "SPC Q Charts for Start-Up Processes and Short or Long Runs". *Journal of Quality Technology* 23, pp. 213–224.

Quesenberry, C. P. (1995). "On Properties of Q Charts for Variables". *Journal of Quality Technology* 27, pp. 184–203.

Reynolds, Jr., M. R. and Stoumbos, Z. G. (2001). "Monitoring the Process Mean and Variance Using Individual Observations and Variable Sampling Intervals". *Journal of Quality Technology* 33, pp. 181–205.

Reynolds, Jr., M. R. and Stoumbos, Z. G. (2005). "Should Exponentially Weighted Moving Average and Cumulative Sum Charts Be Used with Shewhart Limits?" *Technometrics* 47, pp. 409–424.

Shi, J. (2007). *Stream of Variation Modeling and Analysis for Multistage Manufacturing Processes.* Boca Raton, FL: CRC Press.

Stoumbos, Z. G. and Reynolds, Jr., M. R. (2000). "Robustness to Non-Normality and Autocorrelation of Individuals Control Charts," *Journal of Statistical Computation and Simulation* 66, pp. 146–187.

Stoumbos, Z. G. and Sullivan, J. H. (2002). "Robustness to Non-Normality of the Multivariate EWMA Control Chart". *Journal of Quality Technology* 34, pp. 260–276.

Zhang, J. (2002). "Powerful Goodness-of-Fit Tests Based on Likelihood Ratio". *Journal of the Royal Statistical Society, Series B* 64, pp. 281–294.

Zhang, J. (2006). "Powerful Two-Sample Tests Based on the Likelihood Ratio". *Technometrics* 48, pp. 95–103.

Zhou, C.; Zou, C.; Zhang, Y.; and Wang, Z. (2009). "Nonparametric Control Chart Based on Change-Point Model". *Statistical Papers* 50, pp. 13–28.

Zou, C.; Zhou, C.; Wang, Z.; and Tsung, F. (2007). "A Self-Starting Control Chart For Linear Profiles". *Journal of Quality Technology* 39, pp. 364–375.